



Effect of dye structure on color removal efficiency by coagulation

Felix Mcyotto^a, Qunshan Wei^{a,*}, Daniel K. Macharia^b, Manhong Huang^a, Chensi Shen^a, Christopher W.K. Chow^c

^a College of Environmental Science and Engineering, Donghua University, Shanghai 201620, China

^b State Key Laboratory for Modification of Chemical Fibers and Polymer Materials, International Joint Laboratory for Advanced Fiber and Low-Dimension Materials, College of Material Science and Engineering, Donghua University, Shanghai 201620, China

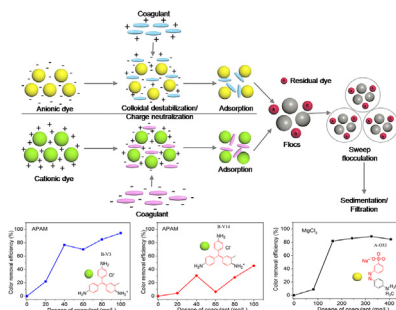
^c Scarce Resources and Circular Economy (ScaRCE), UniSA STEM, University of South Australia, Mawson Lakes, SA 5095, Australia



HIGHLIGHTS

- Dye structures and color removal efficiency by coagulation process are interconnected.
- Dyes with same chromophores and auxochromes can be coagulated with same coagulant effectively.
- Dyes with azo chromophores –OH auxochromes are effectively removed by $MgCl_2$.
- Reactive dyes with phthalocyanine chromophores are effectively removed by PAC.
- Basic dyes can only be removed effectively by anionic coagulants.

GRAPHICAL ABSTRACT



ARTICLE INFO

Keywords:

Dye structures
Color removal efficiency
Coagulation dosage
Dye test solutions

ABSTRACT

The color removal efficiencies by coagulation of two groups of laboratory-prepared dye solutions were compared; one group comprised dyes with the same chromophores and auxochromes, and the other group consisted of dyes with different chromophores and the same or different auxochromes. Several coagulants, polyaluminum chloride (PAC), cationic polyacrylamide (CPAM), anionic polyacrylamide (APAM), aluminum sulfate (alum as $Al_2(SO_4)_3$), ferric chloride ($FeCl_3$), aluminum chloride ($AlCl_3$), and magnesium chloride ($MgCl_2$), were selected to cover a large range of experimental variations in order to obtain sufficient data to predict and model the color removal efficiency. The effect of coagulant dosage on the color removal efficiency was determined, and the dye removal mechanism by coagulation was further investigated using the best performing coagulants for each dye group (disperse, acid, reactive, and basic). It was shown that the best dye–coagulant combinations that achieved superior color removal efficiency for each dye group with the same structures and functional groups were disperse dye– $MgCl_2$ at a pH of 12, acid dye– $MgCl_2$ at a pH of 12, reactive dye–PAC at a pH of 7.5, and basic dye–APAM at a pH of 8.3, in descending order. When treated with the same coagulant, dyes with the same auxochromes and charge exhibited very similar color removal efficiency. The state of the dye molecules in water was shown to have a significant influence on the coagulation effect. The experimental results indicated that the dye color removal efficiency by coagulation is a function of the dye structures.

* Corresponding author.

E-mail address: qswei@dhu.edu.cn (Q. Wei).

<https://doi.org/10.1016/j.cej.2020.126674>

Received 29 January 2020; Received in revised form 30 July 2020; Accepted 12 August 2020

Available online 14 August 2020

1385-8947/ © 2020 Elsevier B.V. All rights reserved.

1. Introduction

Textile manufacturing processes consist of various processing stages that require the use of a combination of chemicals and water [1,2]. These processing stages generate large volumes of wastewater [3,4] and involve complex chemical substances as process residuals, such as dyes. Thus, the textile industry is considered one of the most polluting industrial sectors [5]. Increased global focus on environmental protection and public awareness have resulted in tougher environmental regulations and legislation in many countries. To meet these stringent environmental protection statutory and regulatory requirements, greater efforts from scientists and engineers are required [6].

The wastewater generated from textile factories because of residual materials is characterized by its high biological oxygen demand (BOD), chemical oxygen demand (COD), color intensity, temperature, pH, toxicity, and turbidity [7,8]. Modern commercial dyes also have the characteristics of strong color [9] and structural stability imparted by extensive chromophore conjugation, synthetic origin, and high degree of aromaticity [10-12]. This effluent has very low biodegradability because it contains dye types that have complex structures [13] and high molecular weights [14] (e.g., plant components such as lignin, tannin, and melanoidin [15]). Disposal of this wastewater directly into the receiving water bodies can be toxic to aquatic life [16,17] and can negatively impact flora and fauna [18,19]. Because these compounds may be carcinogenic and mutagenic, they pose serious health risks to human beings [13,20]. In addition, undesirable color changes of the waste caused by the dyes can inhibit sunlight penetration and deplete dissolved oxygen in the water, consequently reducing photosynthetic activity [20].

Various physical, biological, and chemical techniques are used to remove dye from textile wastewater [3,21-24], which include photocatalytic degradation [25], catalytic ozonation [26,27], biological treatment [28-32], adsorption [33], ion exchange [34,35], electrocoagulation [8,36], membrane filtration [9,37], combined chemical and biological processes [38], advanced oxidation processes [39], coagulation-flocculation [20,24], electrochemical oxidation [7], and the Fenton process [40]. The performance of these treatment technologies depends upon their application and is also influenced by the type of textile effluents [41-43]; dye stability towards light and oxidizing agents complicates the treatment of textile effluents [13]. For instance, the widely used conventional biological treatment process is largely effective in handling suspended solids, BOD, and color (dyes are highly adsorbed onto activated sludge). Nevertheless, this process is limited in use because of longer treatment durations, the large operational space needed, the toxicity and recalcitrant nature of dyes, etc. [8,44]. The adsorption process has been reported to exhibit high color removal efficiency and adsorbent regeneration ability [4]. However, its application is restricted by sludge generation and high adsorbent disposal costs [3]. OH radicals generated by the electrochemical advanced oxidation method are effective in oxidizing unsaturated and saturated compounds [45]. Unfortunately, this process has low stability and high operating costs. In terms of process selection for removal of color from textile effluents, coagulation is well established and among the most widespread chemical-physical water treatment processes [21,46]. It has been used for many years either as a pretreatment or main treatment because of its low capital cost [47], simplicity in operation, and high efficiency [48,49].

A single method of treatment is inadequate for decolorization of textile effluents because of their complex and recalcitrant nature. Therefore, hybrid processes integrating multiple treatment processes into a single one have gained considerable attention and are actively being developed [38,50]. Su and Liang et al. [38,51] reported that a combination of coagulation and nanofiltration is able to treat high concentrations of several dyes in wastewater with production of low amounts of sludge. Sun et al. also reported that coagulation is widely employed in enhanced primary, biological, and advanced urban

sewerage treatment [52]. The complexity of industrial textile wastewater and the current focus on hybrid/combined processes make the coagulation and flocculation process a viable and appropriate treatment technology for textile wastewater. The importance of coagulation as a part of the combined treatment process has led to research and development focus being placed on flocculation technology, and the synthesis of new coagulants (e.g., polysilicate ferric manganese (PSFM) [50]); many newly synthesized, low cost and highly efficient coagulants have appeared in recent years [52]. This has led to the emergence of some new explanations on the efficiency of flocculants/coagulants for the treatment of effluents with specific water quality, such as surface complexation based exclusive adsorption, net-sweeping, and organic matter micelle adsorption [52,53]. However, the advancement of synthesis technology has compounded the choice of appropriate coagulants as it focusses on specific dye types [54]. Thus, the choice of an appropriate coagulant remains essential and critical for improving water quality and reducing environmental impacts.

Several studies have been conducted in the recent past on coagulation of real and synthetic textile effluents [44], using various common and widely available inorganic chemicals, such as polyferric sulfate (PFS), polyferric chloride (PFC), polyaluminum chloride (PAC), cationic polyacrylamide (CPAM), anionic polyacrylamide (APAM), aluminum sulfate ($\text{Al}_2(\text{SO}_4)_3$), ferric chloride (FeCl_3), aluminum chloride (AlCl_3), magnesium chloride (MgCl_2), and lime [19]. Yadav and El-Gohary et al. [44,55] reported that MgCl_2 and FeSO_4 could potentially remove 85–100% color from dye effluents at very high alkaline conditions. Similar studies in the existing literature have also examined the effects of pH, coagulant dosages, stirring rate, flocculation time, settling time, and coagulant aids on color removal efficiency [5,6,47-50,56-60]. Optimization of the coagulation process requires effective regulation of these factors. For instance, it has been shown that the color removal efficiency of acid red and reactive blue dyes by MgCl_2 improved with increasing coagulant dosage [60]. Increments in PAC and alum dosages have also been reported to result in increased color removal efficiency [61]. Reactive and disperse dyes have been shown to attain optimum color removal efficiency when the pH was above 12 and MgCl_2 was used as the coagulant [58]. Addition of kaolinite as a coagulant aid in the coagulation/flocculation process (using PAC and alum) has been shown to increase the efficiency of the process, whereas bentonite affected the same process negatively [61]. The critical factors affecting the efficiency of the coagulation process, such as pH, affect the performances of various coagulants differently. Coagulation morphology control involving mainly floc strength, fractal dimension and floc growth [52,62] is also very critical in optimizing the coagulation process. For instance, to ensure good effluent quality and withstand different unfavorable conditions, quality flocs with strong cohesive forces and suitable particle sizes need to be formed [52]. Verma et al. reported that flocculation fractal dimension is linear with floc strength [22]. Moreover, throughout the coagulation process, the flocs' strength is low and decreases with floc size increment [52].

Textile effluents are complex as they contain a mixture of various kinds of dyes; therefore, it is important to characterize the type and structure of dyes in the wastewater before embarking on treatment using coagulation. Appropriate coagulants can then be selected based on the chemical structures and specific coagulation mechanisms of different kinds of dyes; thereafter, coagulation conditions can be optimized with ease.

To the best of our knowledge, limited research has been reported on how the respective dye structures affect the efficiency of color removal from textile wastewater. This study aims to investigate how the chemical structure of dyes is interconnected with the efficiency of color removal by coagulation; understanding this interconnection would be invaluable in choosing the appropriate coagulant for different industrial textile wastewaters and modeling the performance of a particular coagulant for various kinds of dyes with similar or different structures (chromophores and auxochromes).

2. Materials and methods

2.1. Chemicals, dyes, and coagulants

Twenty-three commercial dyes and seven coagulants were obtained from the suppliers and used without any further purification. PAC, CPAM, and APAM were of commercial grade. $Al_2(SO_4)_3$, $FeCl_3$, $AlCl_3$, and $MgCl_2$ were procured from Sinopharm Chemical Reagent Co., Ltd. The dyes were procured from commercial suppliers in China. The real raw reactive dyes effluent containing two reactive dyes was collected from Yixing Leqi Textile Dyeing and Printing, Ltd., located in Yixing City, Jiangsu Province, China. The pH adjustment was performed using NaOH and HCl, which were of reagent grade and procured from Sinopharm Chemical Reagent Co., Ltd.

2.2. Experimental procedure

Each of the 23 dyes were used for the preparation of their own laboratory dye test solution by adding 1 g of the dye to 10 L of deionized water. The real raw reactive dyes wastewater (RRD-WW) was diluted to a ratio of 1:1,000 to prepare real raw dye test solution. Laboratory tests were conducted on the test solutions of the 23 dyes and the RRD-WW test solution samples. The synthetic dye test solutions were used to examine how the dye structures were related to the color removal efficiency of various coagulants for different dye types; the aim was that the use of pure dye test solutions would make it possible to obtain this information. The name, chromophoric group, and maximum absorbance wavelength of each of the 23 dyes and the two dyes in the RRD-WW used for this study are given in Table 1. The molecular structures of the same dyes (Table S5) and the physiochemical parameters of the raw reactive dyes textile effluent (Table S1) are provided in the supporting information section.

The optimum dosages of coagulants required for color removal were determined by the jar testing procedure at room temperature (25 ± 2 °C) to optimize the set experimental parameters (pH, stirring rate, and flocculating time). The optimum pH values were set as per previous research [22,63], as shown in Table 2. Next, 200 ml of each

Table 1

Dye Characteristics – Chromophoric group and maximum absorbance wavelength.

Name	Chromophoric group	Wavelength absorbed (nm)
Disperse red (D-RD)	Azo	459
Disperse black (D-BK)	Azo	578
Disperse blue (D-BE)	Azo	596
Disperse yellow–brown (D-YB)	Azo	281
Acid green (A-GN)	Azo	638
Acid orange 20 (A-O20)	Azo	511
Acid orange 52 (A-O52)	Azo	434
Acid orange74 (A-O74)	Azo	477
Acid red (A-RD)	Azo	511
Acid yellow 36 (A-Y36)	Azo	441
Acid chrome blue k (A-CBK)	Azo	552
Acid fuchsin (A-FN)	Triarylmethane	306
Acid blue 93 (A-B93)	Triarylmethane	630
Acid lake blue (A-LB)	Triarylmethane	589
Reactive Turquoise Blue (R-TB)	Phthalocyanine	611
Reactive yellow 18 (R-LY)	Azo	423
Reactive black 5 (R-BK)	Azo	620
Reactive red (R-BR)	Azo	534
Basic blue 9 (B-BE)	Anthraquinones	594
Basic violet 14 (B-V14)	Triarylmethane	543
Basic violet 10 (B-RD)	xanthene	524
Basic green 4 (B-GN)	Triarylmethane	618
Basic crystal violet (B-CV)	Triarylmethane	582
Reactive Blue X-BR (RBX-BR)	Azo	204
Reactive Red X-3B (RRX-3B)	Azo	204

Table 2

Optimum coagulation pH of selected coagulants used by different researchers.

Name of Coagulant	Optimum pH	Applied pH	Reference
Alum	5.7–7.0	5.7	[76–78]
$AlCl_3$	6.5	6.5	[79]
$FeCl_3$	6.0	6.1	[45,80]
$MgCl_2$	12.0	12	[48,53]
PAC	7.5–8.0	7.5	[20,81]
CPAM	7.8	7.8	[82]
APAM	8.3	8.3	[83]

100 mg/L dye test solution, contained in a 250 ml beaker, was placed on a six-position mechanical stirrer. A period of 1 min was allowed for the rapid mixing of the coagulants and dye test solutions at 300 rpm, followed by slow mixing at 50 rpm for 10 min. The solutions were then allowed to settle for 30 min. After settling, an aliquot of supernatant was pipetted from each jar and then filtered using a 0.45 μ m membrane prior to analyses. A UV spectrophotometer (Analytik Jena SPECORD 200 PLUS) was used to quantify the color residual after treatment. For each absorbance measurement, the maximum absorbance wavelength (λ_{max}) of each dye was employed. The precipitates from the treated dye test waters were filtered and then neutralized and re-dissolved by acidification to become solution. The Analytik Jena SPECORD 200 PLUS was then used for spectral analysis of these precipitates. Portions of the precipitates from the treated wastewaters were filtered, dried, and then analyzed using a Fourier Transform Infrared Spectroscopy (FTIR) meter (Brooktensar 27), a D/MAX-2550/PC X-ray diffractometer (XRD) (Rigaku, Japan), a H-9500 Transmission Electron Microscope (TEM) (Hitachi), and a S-4800 Scanning Electron Microscope (SEM) (Bruker Nano GmbH, Berlin, German). Zeta potential measurement was conducted using a Zeta potential distribution analyzer (Brookhaven NanoBrook 90 Plus PALS, USA).

The percentages of color removal efficiency were calculated by comparing the absorbance value after treatment to the absorbance value for the original dye test solution, as shown by Eq. (1):

$$\text{Color Removal Efficiency (\%)} = \frac{C_0 - C_t}{C_0} \times 100\% \quad (1)$$

where C_0 and C_t are the dye concentrations in the original and treated dye test solutions respectively. Deionized water was used as a reference.

3. Results and discussion

3.1. Effect of coagulant dosage on color removal efficiency

For this study, the coagulation conditions/parameters (mixing time and speed) were kept constant for all the experiments, and the coagulant dosage was chosen as the single variable for comparison. Four dyes (disperse red, acid red, reactive red, and basic red) and seven coagulants (PAC, CPAM, APAM, $Al_2(SO_4)_3$, $FeCl_3$, $AlCl_3$, and $MgCl_2$) were used. Disperse red, acid red, and reactive red dyes have azo chromophores, whereas basic red dye has a xanthene chromophore; this was used at preliminary stages to predict if there was any correlation between the dye structures and the widely used coagulants, as well as how their dosage was affected. Fig. 1 shows the coagulation performances of the seven coagulants with the four chosen dyes. It is clearly shown that with increased dosage of the coagulant, the color removal efficiency increased accordingly. Table 3 summarizes the maximum dye color removal efficiencies (for disperse red, acid red, reactive red, and basic red dyes) by the different coagulants.

Based on these results, $MgCl_2$ achieved the best color removal efficiency of 96.1% at a low dosage of 81.2 mg/L. Subsequent increment of coagulant dosage led to a peak of 96.7% at a dosage of 162.4 mg/L. Further increment of $MgCl_2$ dosage past the peak resulted in decrement of the color removal efficiency. For instance, at a dosage of 406 mg/L,

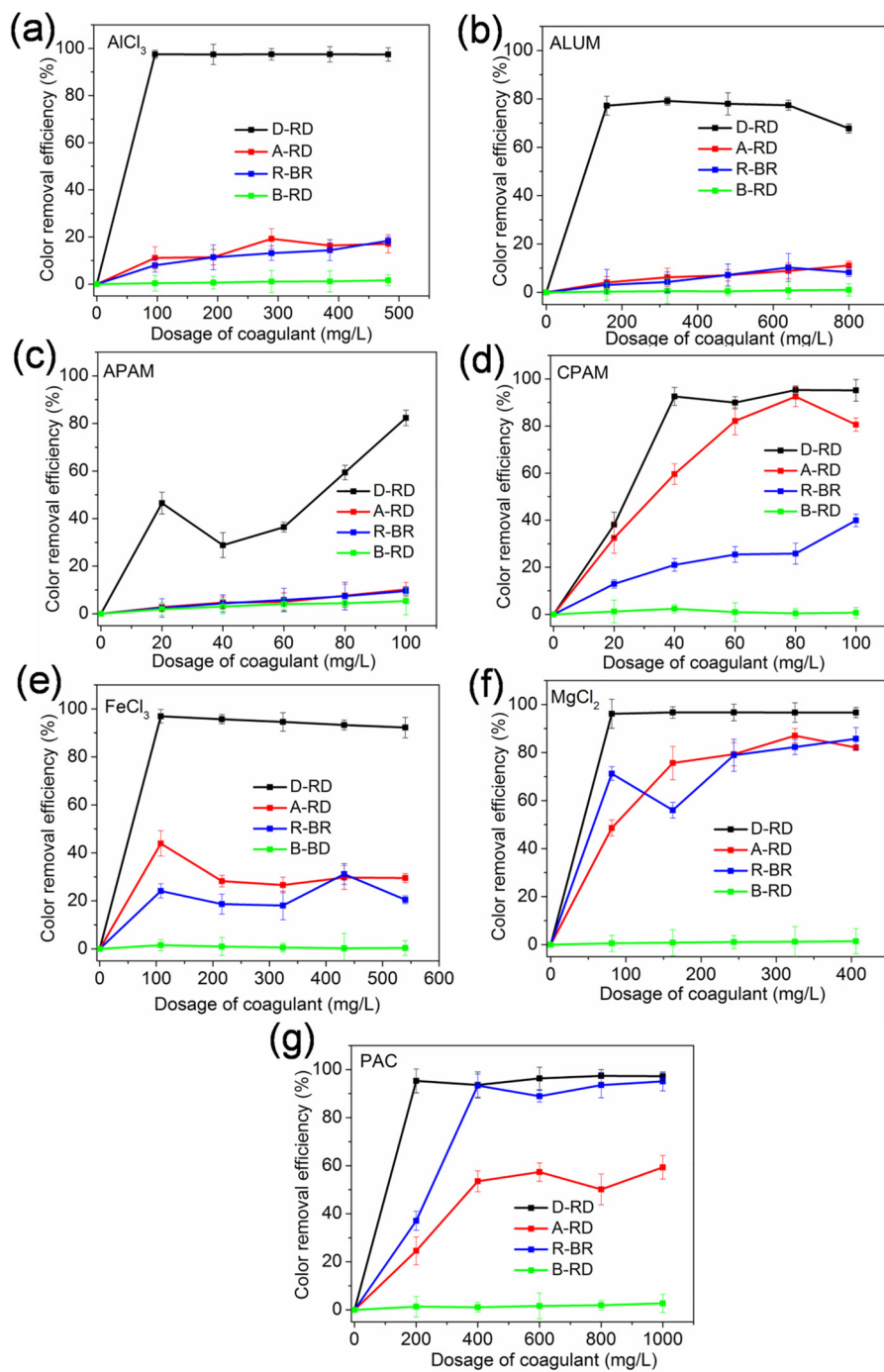


Fig. 1. Effect of coagulant dosage on the color removal efficiency (D-RD is Disperse Red, A-RD is Acid Red, R-BR is Reactive Brilliant Red and B-RD is Basic Red).

Table 3
Effect of coagulant dosage (mg/L)^a on color removal efficiency.

Coagulant Name	Maximum dye removal efficiency (%)			
	D-RD	A-RD	R-BR	B-RD
Al ₂ (SO ₄) ₃	79.1 (320)	11.1 (800)	10.3 (640)	1.0 (800)
AlCl ₃	97.5 (96.4)	19.2 (289.2)	18.4 (482)	1.6 (800)
FeCl ₃	96.9 (108)	43.9 (108)	31.2 (432)	1.6 (20)
MgCl ₂	96.7 (162.4)	87.0 (324.8)	85.5 (406)	1.5 (406)
PAC	97.4 (800)	59.3 (1000)	95.1 (1000)	2.7 (1000)
CPAM	95.3 (100)	92.5 (80)	39.9 (100)	2.4 (40)
APAM	82.4 (100)	10.2 (100)	9.6 (100)	5.3 (100)

^a The figures in parentheses are the coagulant dosages.

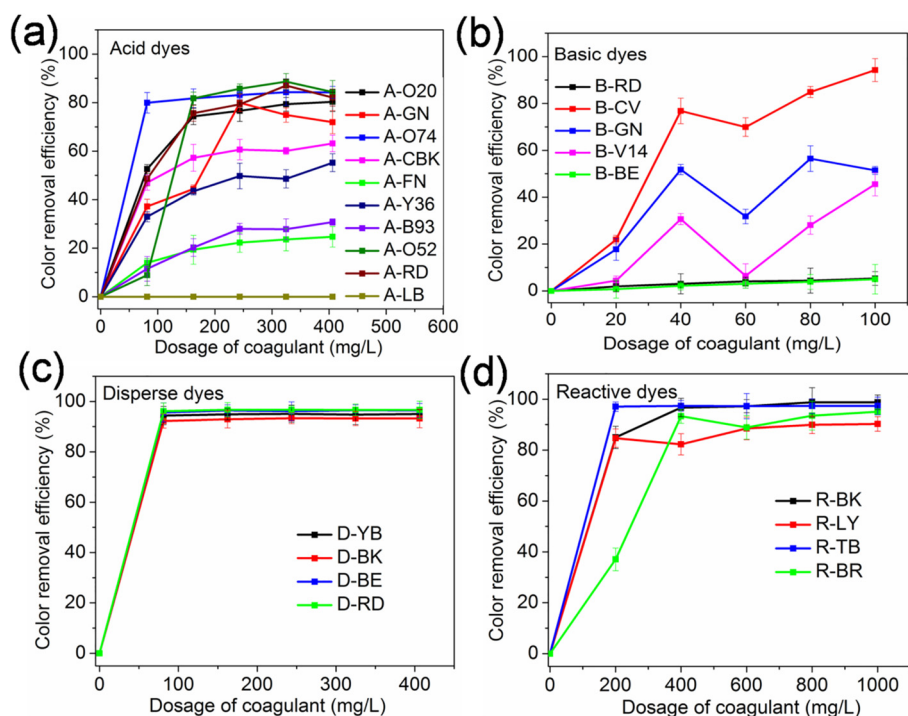


Fig. 2. The comparison of the color removal efficiency by different coagulants as a function of dosage: a) acid dyes treated with $MgCl_2$, b) basic dyes treated with APAM, c) disperse dyes treated with $MgCl_2$, and d) reactive dyes treated with PAC.

$MgCl_2$ achieved a color removal efficiency of 96.6%. In most cases, 95% color removal efficiency could be achieved for disperse red dye when different coagulants were used.

CPAM achieved the best results for acid red at a dosage of 80 mg/L, achieving a color removal efficiency of 92.5%. The lowest color removal efficiency by CPAM was 32.4% at a dosage of 20 mg/L. Increasing the dosage of CPAM increased the color removal efficiency until the peak was attained. Further increment resulted in decrement of the color removal efficiency; that is, at a dosage of 100 mg/L, the color removal efficiency was lowered to 82.1%. $MgCl_2$, in contrast, resulted in the second highest color removal efficiency, 87.0% at a dosage of 324.8 mg/L. $MgCl_2$ exhibited the same phenomenon as CPAM whereby increment of coagulant dosage led to increment of the color removal efficiency until the peak was attained. Any further coagulant dosage increments past the peak led to decrement of the color removal efficiency. For instance, at a dosage of 81.2 mg/L, $MgCl_2$ yielded 48.6% color removal efficiency, whereas at a dosage of 406 mg/L, it yielded a color removal efficiency of 82.1%. In terms of the ease of coagulation, flocculation, and filtration of the aliquot supernatant, $MgCl_2$ exhibited better performance than CPAM.

The best color removal efficiency for reactive brilliant red dye was achieved by PAC. Increment of PAC dosage resulted in subsequent increment of the color removal efficiency. For instance, a PAC dosage of 200 mg/L yielded 37.0% color removal efficiency, whereas 600 mg/L PAC dosage removed 88.9% of the reactive brilliant red color.

The best color removal performance for basic red dye was exhibited by APAM. Increment of the dosage of APAM resulted in increment of the color removal efficiency of the basic red dye. Nevertheless, the color removal efficiency was relatively low. At a 20 mg/L dosage of APAM, only a 2.0% color removal efficiency of basic red dye was achieved. At a 60 mg/L dosage of APAM coagulant, 4.1% color removal efficiency was achieved, whereas at 100 mg/L dosage, 5.3% color removal efficiency was achieved. In all cases, less than 3% color removal efficiency could be achieved for basic red dye when cationic coagulants were used.

The above results indicate that the best dye color removal efficiencies were achieved by $AlCl_3$ for disperse red dye, $MgCl_2$ for acid red

dye, PAC for reactive brilliant red, and APAM for basic red dye. However, $MgCl_2$ at the very low dosage of 81.2 mg/L removed 96.1% of color for disperse red dye, indicating better performance than $AlCl_3$ at lower dosages. It is evident from the results that the best removal efficiency for each dye is dependent on the type of coagulant. The disperse red dye had the best color removal efficiency for all the tested coagulants. Disperse dyes have been reported to coagulate well and settle easily compared with the other types of dyes [64]. The improved coagulation by disperse dyes results from their greater numbers of more polar groups (such as -O- and -NH-) and fewer hydrophilic groups. Disperse red dye has these characteristics, which make it easy to remove by coagulation.

According to the experimental results obtained above, the -OH functional group in the disperse red dye and acid red dye reacts with magnesium ions [58]. This leads to the formation of magnesium hydroxide precipitate, which has a structure that provides a large area for adsorption [60]. It also creates a positive electrostatic charge at the surface. This positive electrostatic charge at the surface and the large cumulative adsorptive surface area enable efficient coagulation [58,60]. PAC exhibits strong bridge adsorptive performance. Its structure consists of a polycarboxyl complex with variable morphology; thus, it reacts easily with the reactive groups (-Cl, -OH, and SO_3Na) in reactive brilliant red dye. Basic red dye has good solubility and is positively charged; thus, it reacts easily with APAM, which is anionic.

3.2. Effect of dye structure on color removal efficiency by different coagulants

From the first phase of the experiments, it was determined that the best dye-coagulant combinations were disperse red dye- $MgCl_2$, acid red dye- $MgCl_2$, reactive brilliant red dye-PAC, and basic red dye-APAM. Consequently, $MgCl_2$ was used for investigation of other disperse dyes and acid dyes, PAC for reactive dyes, and APAM for basic dyes. Each of these dye cluster had a group of dyes with the same chromophores and auxochromes and another group with different chromophores and the same or different auxochromes. The aim was to

Table 4
Comparison of the maximum color removal efficiency of different dye clusters by different coagulants.

Name	Coagulant Name	Maximum dye removal efficiency (%)	
Disperse red (D-RD)	MgCl ₂	96.7	
Disperse black (D-BK)		93.3	
Disperse blue (D-BE)		96.6	
Disperse yellow–brown (D-YB)		95.3	
Acid green (A-GN)	MgCl ₂	79.9	
Acid orange 20 (A-O20)		80.3	
Acid orange 52 (A-O52)		88.7	
Acid orange74 (A-O74)		84.3	
Acid red (A-RD)		87.0	
Acid yellow 36 (A-Y36)		55.3	
Acid chrome blue k (A-CBK)		63.2	
Acid fuchsin (A-FN)	PAC	24.7	
Acid blue 93 (A-B93)		30.8	
Acid lake blue (A-LB)		0.0	
Reactive Turquoise Blue (R-TB)		97.4	
Reactive yellow 18 (R-LY)		90.3	
Reactive black 5 (R-BK)		98.8	
Reactive red (R-BR)		95.1	
Basic blue 9 (B-BE)		APAM	5.0
Basic violet 14 (B-V14)			45.5
Basic violet 10 (B-RD)			5.3
Basic green 4 (B-GN)			56.5
Basic crystal violet (B-CV)	94.3		

establish whether possible/predictable correlation exists between dye color removal efficiency and structure. The results showing the comparison of the color removal efficiency by various coagulants as a function of dosage are presented in Fig. 2. Table 4 compares the maximum color removal efficiencies of different dye clusters by different coagulants.

MgCl₂ showed very good dye color removal efficiency for the four disperse dyes. The results are shown in Fig. 2 (c). However, disperse black dye exhibited a lower color removal efficiency than the rest. All the disperse dyes have same main structure with azo chromophores and auxochromes (–OH and –Cl). The –OH auxochromes in all the four disperse dyes form Mg(OH)₂, which acts through an adsorptive coagulation mechanism. Disperse red, disperse blue, and disperse yellow brown have an additional auxochrome (–S), which suggests that disperse black is more nonionic, and thus has lower color removal efficiency. The –OH auxochrome is the key reason for easy removal of disperse dyes by coagulation using MgCl₂, as the coagulant.

PAC showed very high color removal efficiencies for the four reactive dyes. The results are shown in Fig. 2(d). PAC provided the best color removal efficiency for reactive turquoise blue at the lowest dosage compared with the other three (reactive brilliant red, reactive black 5, and reactive light yellow 18). Reactive turquoise blue has a phthalocyanine chromophore, whereas the other three have an azo chromophore. This explains the easier color removal of reactive turquoise by PAC than the other three reactive dyes. All four reactive dyes contain the same auxochromes (–SO₃Na, –Cl, and –NH₂). The phthalocyanine chromophore is the reason for easier color removal of reactive turquoise blue compared with the other three reactive dyes with azo chromophores by coagulation using PAC; the presence of –SO₃Na, –Cl, and –NH₂ auxochromes also allows easy color removal of reactive dyes by coagulation using PAC.

APAM showed better color removal efficiency for the basic dyes than all the positive ion coagulants. The results are shown in Fig. 2(b). However, it still had low color removal efficiencies for the basic dyes, apart from basic crystal violet dye. This was because basic dyes do not easily coagulate [64]. Basic crystal violet had the highest color removal efficiency, followed by basic green 4 and basic violet 14, whereas basic red 10 and basic blue 9 respectively had the lowest dye color removal efficiencies (shown in Fig. 2(b)). Basic crystal violet, basic green 4, and

basic violet 14 dyes have a triarylmethane chromophore. However, basic green 4 has one more –NH₂ than basic crystal violet, and thus has a more positive charge in solution; NH₂ forms –NH³⁺ in solution. Basic red 10 has a xanthene group chromophore, whereas basic blue 9 has an anthraquinone group chromophore. Therefore, the absence of the –NH₂ auxochrome is key for these dyes to achieve better color removal efficiency by coagulation using APAM.

Moreover, all five basic dyes contain an –NH₂ auxochrome (apart from crystal violet) and an alkyl functional group –Cl. The absence of the –NH₂ in crystal violet explains its higher color removal efficiency than the other basic dyes, as amines increase basicity.

MgCl₂ showed very good dye removal efficiency for five acid dyes (acid green, acid orange 20, acid red, acid orange 52, and acid orange 74). MgCl₂ had moderate color removal efficiency for two other acid dyes (acid yellow 36 and acid chrome blue K). Acid fuchsin and acid blue 93 had very low color removal efficiencies, and acid lake blue exhibited zero color removal efficiency for the same coagulant. The results are shown in Fig. 2(a). Acid fuchsin, acid blue 93, and acid lake blue dyes have triarylmethane chromophore groups, whereas the rest of the acid dyes have azo chromophore groups. They all have –OH and –SO₃Na. However, acid lake blue alone has NH⁴⁺, which indicates why it did not coagulate at all, as this makes it more cationic. Therefore, the azo chromophore is the key group for acid dyes to achieve better color removal efficiency by coagulation using MgCl₂. The presence of triarylmethane chromophore in an acid dye makes its removal by MgCl₂ coagulant difficult.

The disperse dyes, acid dyes, and reactive dyes have acidic functional groups (such as –OH, –SO₃Na, –Cl, –O–, and –NH–) which can coordinate with metal ions to form relatively hydrophobic complexes. These hydrophobic complexes can easily be removed by coagulation. In contrast, basic dyes have basic functional groups and thus do not easily coagulate.

3.3. Spectral analysis and investigation of the mechanism of color removal by coagulation

For this experiment, disperse red, acid red, reactive turquoise blue, and basic crystal violet dyes were chosen. These dyes had the best color removal efficiencies in their cluster groups. The spectra for the untreated dye test water and supernatant from treated dye test water were analyzed. The precipitates from the treated dye test waters were filtered and then neutralized by acidification to re-dissolve them into solution [60]. The solutions obtained from the precipitates had same colors as the original test dye solutions. A UV spectrophotometer was used to analyze the samples. Fig. 3 shows the obtained results. According to these results, the supernatant aliquots exhibited no characteristic dye color peaks for wavelength ranges of 200 nm to 900 nm, as shown by Fig. 3. This result suggests the transfer of dye from the dye test solution by coagulation into the precipitate, and thus that the dye was easily separated from the liquid [58]. Untreated dye solutions and neutralized precipitate solutions appeared to have identical characteristics, apart from the differences in absorbance (shown in Fig. 3). The untreated dye solutions and the neutralized precipitate solutions had different concentrations. These differences in concentration caused differences in absorbance between the two solutions. The above results indicate that coagulation did not change the molecular structure of the dyes, but rather transferred the dyes from the solution into the precipitate, which could easily be removed [58].

3.4. Effect of zeta potential change on dye color removal efficiency by coagulation

Fig. 4 shows the results of zeta potential measurement of combinations of disperse red dye with AlCl₃, acid red dye with MgCl₂, reactive turquoise blue dye with PAC, and basic crystal violet dye with APAM coagulation processes. These combinations were chosen from

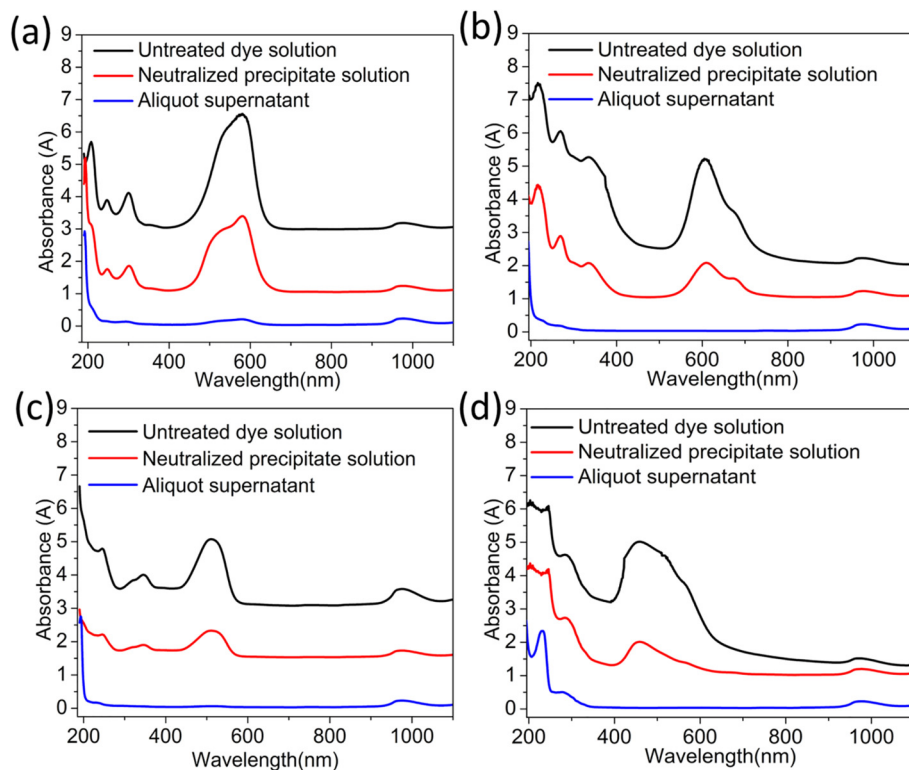


Fig. 3. The spectrogram comparison of different dye-coagulant combinations as a function of color removal mechanism by coagulation process: a) basic crystal violet dye treated with APAM, b) reactive turquoise blue treated with PAC, c) acid red dye treated with $MgCl_2$, and d) disperse red dye treated with $AlCl_3$.

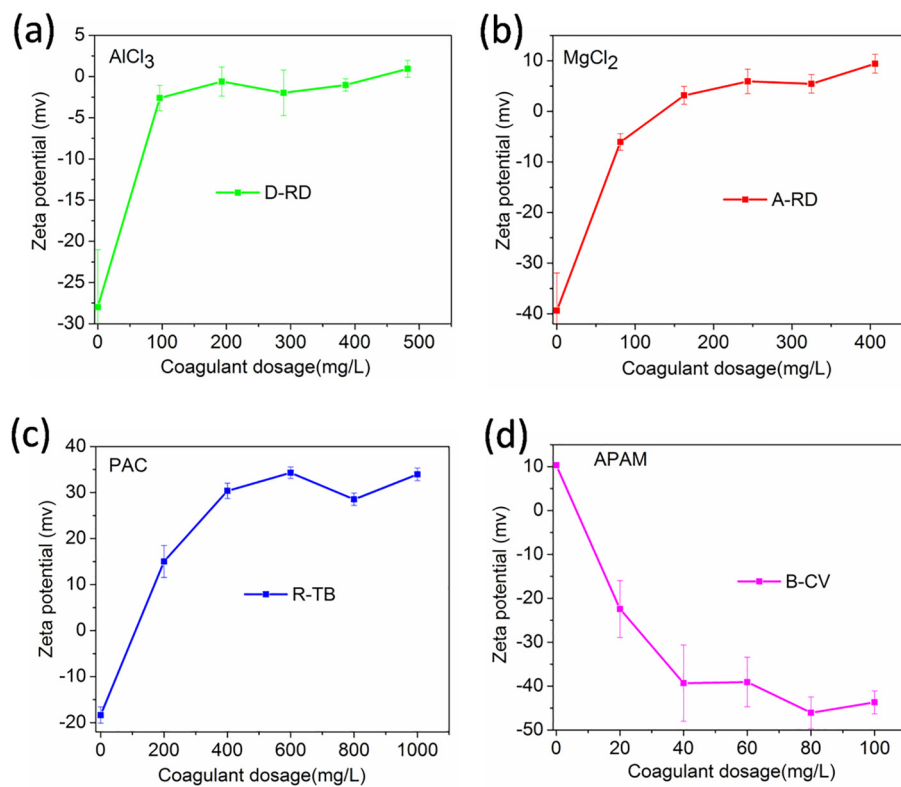


Fig. 4. The effect of coagulant dosage on zeta potential: a) disperse red dye treated with $AlCl_3$, b) acid red dye treated with $MgCl_2$, c) reactive turquoise blue treated with PAC, and d) basic crystal violet dye treated with APAM.

hindsight as they achieved the best color removal efficiencies at low dosages. The zeta potentials of disperse red dye, acid red dye, and reactive turquoise dye increased with increased coagulant dosage (Fig. 4a–c). In contrast, the zeta potential of basic crystal violet dye declined with increase in coagulant dosage because of its cationic nature. These results indicate that the coagulants could induce coagulation through charge neutralization [65]. It has been reported that if the zeta potential value is close to zero and the optimal coagulation/flocculation efficiency is achieved, then excess coagulant dosage will result in charge reversal; thus, the efficiency of coagulation/flocculation will be decreased [65]. The results of this study (Fig. 4) indicate that charge neutralization was not the sole mechanism of coagulation for AlCl_3 , MgCl_2 , PAC, and APAM. However, it played a major role in the disperse red dye– AlCl_3 and acid red dye– MgCl_2 combinations (Fig. 4a–b) as their zeta potentials for various coagulant dosages were mostly close to zero [66].

The zeta potential for disperse red dye for the applied dosages of AlCl_3 was between -2.61 mV and 0.93 mV, whereas that of acid red dye was between -6.04 mV and 9.42 mV for the applied dosages of MgCl_2 . The zeta potential for the reactive turquoise blue dye–PAC combination for the applied dosages of PAC, in contrast, was between 15.03 mV and 33.97 mV. For the basic crystal violet dye–APAM combination, the zeta potential for the applied dosages of APAM was between -22.43 mV and -43.69 mV. According to Kumar et al., colloids with zeta potential between 0 and ± 5 mV exhibit rapid coagulation or flocculation stability behavior, those between ± 10 and ± 30 mV exhibit incipient instability, those between ± 30 and ± 40 mV exhibit moderate stability behavior, and those between ± 40 and ± 60 mV exhibit good stability behavior [67]. This agrees with our zeta potential results in relation to the comparison of the effect of the coagulant dosage on dye color removal efficiency.

3.5. Analysis of coagulation precipitates by FTIR and XRD

The disperse red dye– AlCl_3 , acid red dye– MgCl_2 , and reactive turquoise blue dye–PAC combinations achieved the highest color removal efficiencies at low dosages; therefore, these combinations were chosen for both the FTIR and XRD tests to further clarify the internal mechanisms of the dye and coagulant combinations. Fig. 5 shows the FTIR and XRD analysis results.

FTIR is vital in the study of chemical properties and component stereo structures of materials. Comparison of the infrared spectra of the dyes and their precipitates revealed absorption peaks at $3,300$ – $3,500$ cm^{-1} (Fig. 5a–c) caused by stretching vibration of hydroxyl groups [68]; these hydroxyl groups exist either in a free state or in a contiguous state with metal ions, implying that reactions occurred between the coagulants and the metal ions [69]. The adsorption peaks at $1,620$ – $1,650$ cm^{-1} (Fig. 5a–c) are attributed to bending vibration of hydroxyl groups. Liu et al. describes this peak as variable angle vibration resulting from absorbed water, crystal water, and coordinated water [69]. The pure dyes and the dye–coagulant (floc) patterns at these two peaks appeared basically the same, apart from the slight weakening due to the floc formation. This can be ascribed to the change in hydrogen bonding caused by the reaction of the coagulants with the dyes. The absorption bands of the precipitates at 584 cm^{-1} (Fig. 5a) and 563 cm^{-1} (Fig. 5c) for AlCl_3 and PAC, respectively, correspond to characteristic Al–O absorption peaks (bending and stretching vibrations), whereas the low-frequency region bands for MgCl_2 of 515 cm^{-1} and 439 cm^{-1} (Fig. 5b) correspond to bending and stretching vibrations of Mg–O bonds (MgO translational modes) [19]. These FTIR results indicate the formation of new chemical species due to coagulation [69].

The XRD results (Fig. 5d) indicate the presence of elemental Al and O in the sub-formula of the dye– AlCl_3 precipitate and the presence of elemental Cu and O in the sub-formula of the dye–PAC precipitate. They also show the presence of elemental Mg and O in the sub-formula

of the dye– MgCl_2 precipitate. These results indicate that the precipitates are newly formed chemical species, which is an occurrence generally consistent with the FTIR results. The XRD and FTIR results show that the removal of disperse red dye by AlCl_3 , acid red dye by MgCl_2 , and reactive turquoise blue dye by PAC involves specific chemical binding between dyes and coagulants. Thus, dyes with the same/similar structures and chemical properties will exhibit similar color removal efficiency, which is an assertion consistent with the findings of the optical analysis (shown in Fig. 2).

3.6. Structural and morphological characteristics of coagulation precipitates

SEM and TEM were used to investigate the morphology of coagulation precipitates (disperse red dye– MgCl_2 , acid red dye– MgCl_2 , and reactive turquoise blue dye–PAC) to determine the coagulation mechanism (Fig. 6). The SEM images (Fig. 6a and 6d) indicate that the disperse red dye– MgCl_2 and acid red dye– MgCl_2 coagulation precipitates were composed of aggregated nanoparticles that adhered to fibrous structures. In contrast, the reactive turquoise blue dye–PAC coagulation precipitate was composed of irregularly shaped nanoparticles with the coagulation precipitate as the coating layer (Fig. 6g). These findings indicate that coagulation caused the dyes to adhere onto the surfaces of the nanoparticles to form the precipitates.

To further confirm the presence of flocs on the coagulant nanoparticles, elemental distribution patterns of precipitates after coagulation were determined by energy dispersive spectroscopy (EDS) (Fig. 6b, 6e, and 6h). The EDS elemental distribution mixture shows that the disperse red dye– MgCl_2 precipitate was composed of Mg, Na, Si, Cl, and C; the acid red dye– MgCl_2 precipitate was composed of Mg, Na, Si, Cl, S, and C, whereas the reactive turquoise blue dye–PAC precipitate was composed of Al, Na, Si, Cl, S, and C. Table S2 shows the elemental components derived from the dyes and coagulants. Thus, EDS can confirm the presence of good distribution of dyes on the coagulants, indicating the adsorption of the dyes on the surfaces of the coagulants.

TEM images indicate that the disperse red dye– MgCl_2 , acid red dye– MgCl_2 , and reactive turquoise blue dye–PAC combinations were composed of cherry-like, irregularly shaped, and aggregated nanoparticles, respectively (Fig. 6c, 6f, and 6i). Therefore, it is reasonable to conclude that the dyes adhered to the surfaces of the coagulant nanoparticles by adsorption.

3.7. Mechanism of color removal by coagulation

To better understand the mechanism of dye color removal by coagulation taking place between coagulants and different dye structures, a preliminary depiction of the process is proposed in Fig. 7. MgCl_2 was used at a pH of 12 in the removal of both disperse and acid dye colors (Fig. 2a and 2c). At high pH all Mg^{2+} was likely converted to magnesium hydroxide precipitate. Boon et al. proposed that the solubility constant of magnesium hydroxide precipitate causes its formation from magnesium ions at pH values greater than 10.5 [47]; the $\text{Mg}(\text{OH})_2$ solubility is given by:

$$K_{sp} = [\text{Mg}^{2+}][\text{OH}^-]^2 \quad (2)$$

where K_{sp} denotes the dissociation constant of hydroxide. The formation of the hydroxide precipitate is favored by increase in either Mg^{2+} or OH^- concentration. With removal rates of more than 90% for the disperse dyes (Fig. 2c), conversion of Mg^{2+} to hydroxide precipitate has probably occurred. Leentvaar et al. proposed that this magnesium hydroxide precipitate functions through the mechanism of adsorptive coagulation [70]. Owing to its structure, it has a large surface area for adsorption. This, together with the positive electrostatic charge on its surface, enhances its efficiency as a coagulant [47,58]. It is therefore proposed that the disperse and acid dyes were removed using MgCl_2 through a charge neutralization mechanism, sweep flocculation, and an

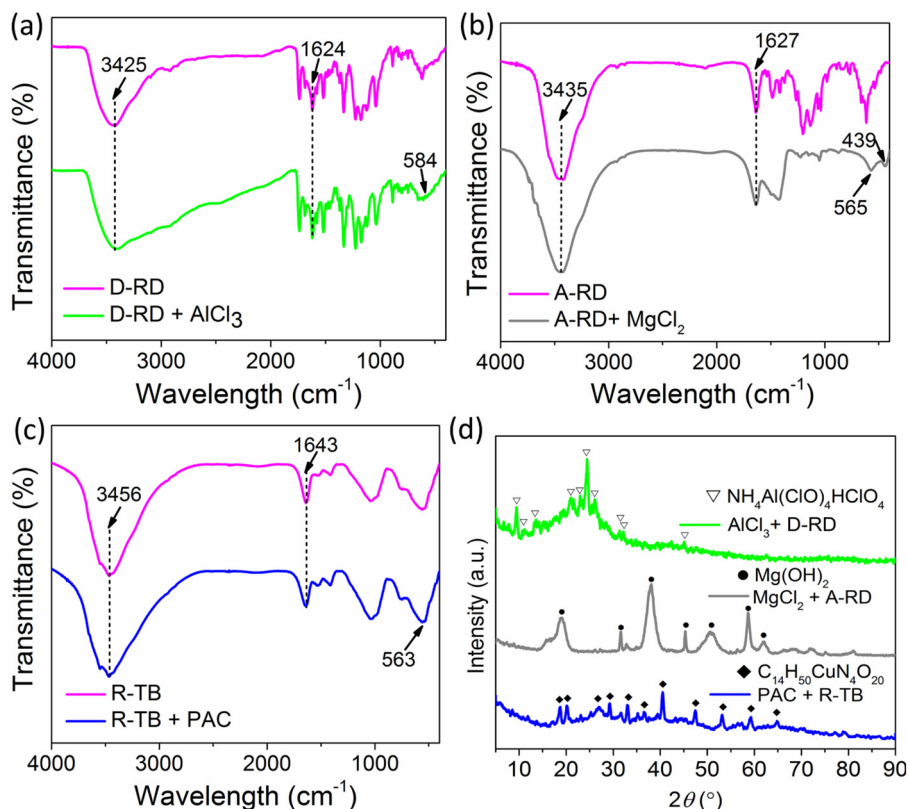


Fig. 5. The FTIR spectra: a) disperse red dye treated with AlCl_3 , b) acid red dye treated with MgCl_2 , c) reactive turquoise blue treated with PAC, and d) XRD patterns of precipitates.

adsorptive coagulation mechanism. This inference also agrees with the findings obtained via FTIR, XRD (Fig. 5), SEM-EDS, and TEM (Fig. 6) analyses, indicating that a new chemical species was formed as a result of specific chemical binding between the dye and coagulant.

Reactive dyes have anionic functional groups; thus, their dissolution in water releases negative charges [61], as shown in Fig. 4c. This confirms that charge neutralization mechanism plays a role in the decolorization of these dyes in solution. The negative charges on the dye molecules are probably neutralized by the hydrolyzed products of the PAC coagulant. Decrease in pH has been reported to cause reduction of the charge density, leading to self-aggregation of the dye molecules [71]. However, it has been reported that PAC attained maximum efficiencies at a pH of 7 and that any reduction in pH leads to decline of coagulation [61]. In this study, PAC was used at a pH of 7.0–7.5.

With charge neutralization, when a certain critical coagulant concentration is reached, the maximum color removal efficiency is attained; thus, further increase of coagulant dosage is expected to cause the suspension to re-stabilize and result in color removal reduction. The obtained results shown in Fig. 2d and Fig. 4c showed otherwise. Therefore, it seems that charge neutralization alone was not responsible for color removal of the reactive dyes using PAC. Sweep flocculation and bridge adsorption mechanism could also be occurring either individually or together. However, because of the polymeric properties of PAC, sweep flocculation and bridge adsorption mechanism could be more likely the dominant mechanism. This also agrees with the FTIR, XRD (Fig. 5), SEM-EDS, and TEM (Fig. 6) findings indicating that a new chemical species was formed, resulting in specific chemical binding between the dye and coagulant.

Basic dyes are cationic; thus, their dissolution in water releases positive charges, as shown in Fig. 4d. The inorganic salts and CPAM could not easily coagulate the basic dyes as they are also cationic (Fig. 1). In contrast, APAM, being anionic in nature, was able to induce

coagulation of the basic dyes. Increase in coagulant dosages led to reduction in zeta potential, and thus increase in the color removal rate for all five basic dyes. Based on this finding, we propose that basic dyes were removed partly through a charge neutralization mechanism. However, with the increase of coagulant dosage, there is an increase in negative charges, signified by great reduction in zeta potential values; that is, further from 0 mV, as shown in Fig. 4d. There was still increase in color removal efficiency with the reduction of zeta potential resulting from increase in coagulant dosage. Therefore, sweep flocculation and bridging adsorption could also be occurring alongside charge neutralization [13].

3.8. Color removal of raw reactive dyes wastewater by coagulation

Real raw reactive dyes wastewater (RRD-WW) samples were used to test and validate the potential and full-scale application of the choice of appropriate coagulant, for decolorization of dye wastewater based on dye structure considerations. The RRD-WW contained two reactive dyes: Reactive Blue X-BR and Reactive Red X-3B. These two dyes have the same chromophore (azo) and auxochromes (SO_3Na , $-\text{Cl}$, and $-\text{NH}_2$). Based on earlier studies, it was shown that PAC had the best color removal performance for reactive dyes, whereas APAM had the worst color removal performance among the seven coagulants used (Fig. 1). Therefore, the RRD-WW was subjected to coagulation using PAC and APAM.

The results showed that coagulation using PAC was effective in decolorization of the reactive dye effluents (Fig. 8). PAC achieved the best color removal efficiency of 78% at a dosage of 400 mg/L, which was higher than the value achieved with the existing conventional treatment methods applied in textile industry effluents [4]. This matches well with the results obtained with the synthetic reactive dye test solutions (reactive brilliant red, reactive black 5, and reactive light

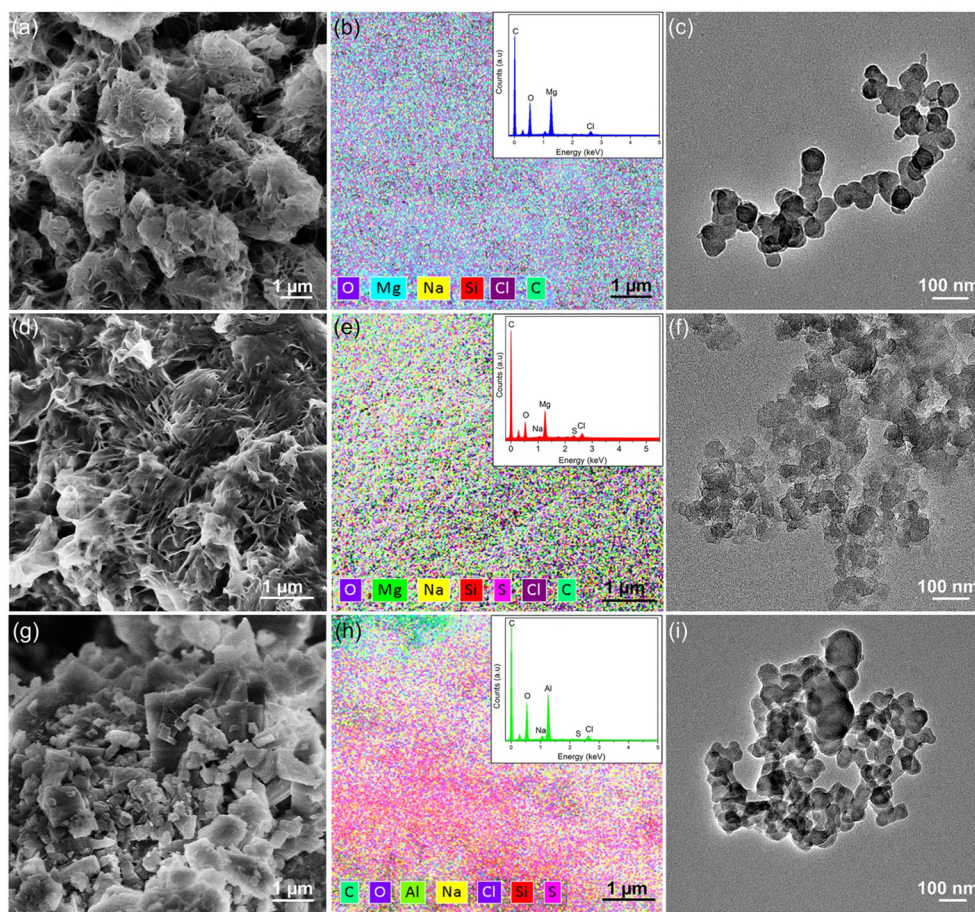


Fig. 6. SEM images (a, d and g), elemental mapping (insets: EDS patterns) (b, e and h), and TEM images (c, f and i) of disperse red dye-MgCl₂, acid red dye-MgCl₂, and reactive turquoise blue dye-PAC coagulation precipitates.

yellow 18 dyes) that have the same chromophore (azo) and auxochromes (SO₃Na, -Cl and -NH₂) as the two dyes in the RRD-WW.

In contrast, APAM achieved color removal efficiency of below 14% across all administered dosages, which indicates that it is ineffective for decolorizing reactive dye wastewater. These findings emphasize that coagulation using the right coagulant is effective in removing soaps, surfactants, metallic ions, and color from textile effluents. Furthermore, the simplicity and low cost of operation of this method make it viable to be used either alone or combined with other processes with various limitations (e.g., electrochemical oxidation and adsorption) (Tables S3 and S4) for pretreatment/post-treatment of textile industry effluents [2,7].

4. Conclusions

In this paper, the direct reactions between 23 dyes with known chemical structures and 7 different coagulants were studied to reveal the effects of dye structures on the coagulation performance, which was also verified by real raw wastewater (from a dyeing and printing company). MgCl₂ removed color effectively from wastewater containing disperse dyes with azo chromophores and auxochromes (-OH and -Cl). PAC removed color effectively from reactive dye wastewater containing phthalocyanine and azo chromophores, with the same auxochromes (-SO₃Na, -Cl, and -NH₂). PAC also effectively removed color from the real raw reactive dyes wastewater, with removal efficiency as high as 78%. This indicates that PAC can effectively decolorize raw real textile effluents containing reactive dyes with azo chromophores and -SO₃Na, -Cl, and -NH₂ auxochromes. Basic dyes are positively charged, and thus generally exhibited very low removal

efficiency with the positive ion coagulants. APAM, a negative ion coagulant, showed better removal efficiency than the positive ion coagulants for basic dyes. The most important mechanisms for disperse, acid, reactive, and basic dye removal by coagulation are charge neutralization, sweep flocculation, and bridge adsorption.

The state of dye molecules in solution has a considerable influence on color removal efficiency by coagulation. If the dye structure contains fewer hydrophilic groups and more polar groups, the solution is suspended or colloidal, and thus is easy to coagulate and remove, as in the case of disperse dyes. If there are charged groups such as -NH-, -NH₂, and -SO₃H in the dye structure, they affect the electrical properties of the dye. This affects the neutralization reaction between the coagulant and the dye, which in turn affects the coagulation.

The experimental results of this study indicate that there is an interconnection between dye structures and the dye color removal efficiency by coagulation. It was shown that dyes with the same or similar characteristics, such as auxochromes and charge, have very close color removal efficiencies when treated with the same coagulant type. Therefore, this work provides a reference for structural considerations of dyes when choosing the most appropriate coagulant for textile wastewater treatment, as well as modeling of the same. More studies with a wider range of dyes and newly synthesized coagulants need to be conducted, thus enabling the development of models that can be used to easily predict the appropriate coagulant for decolorizing any textile effluent based on the structures of the dyes it contains.

Declaration of Competing Interest

The authors declare that they have no known competing financial

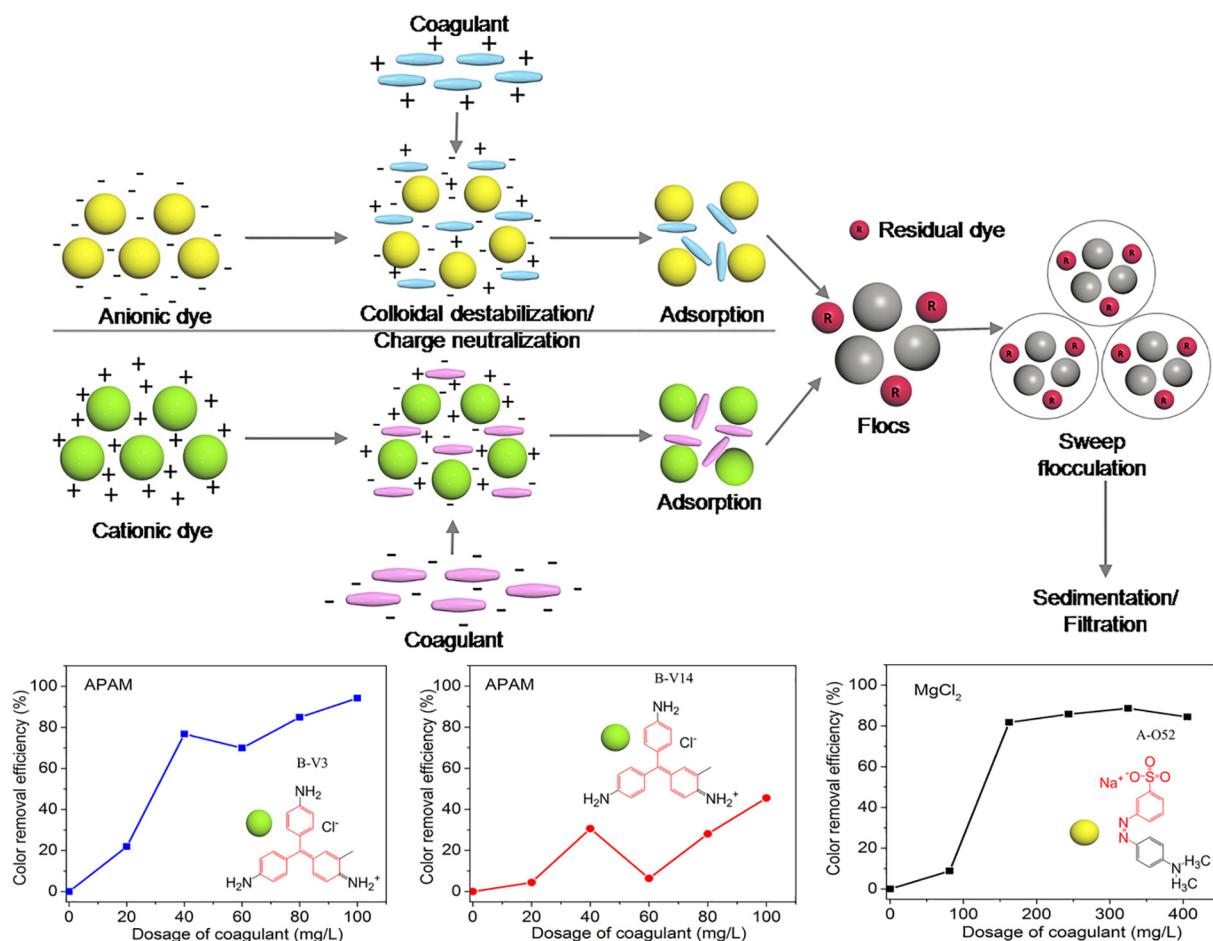


Fig. 7. Scheme illustrating the proposed coagulation mechanism taking place between the coagulants and different dye structures.

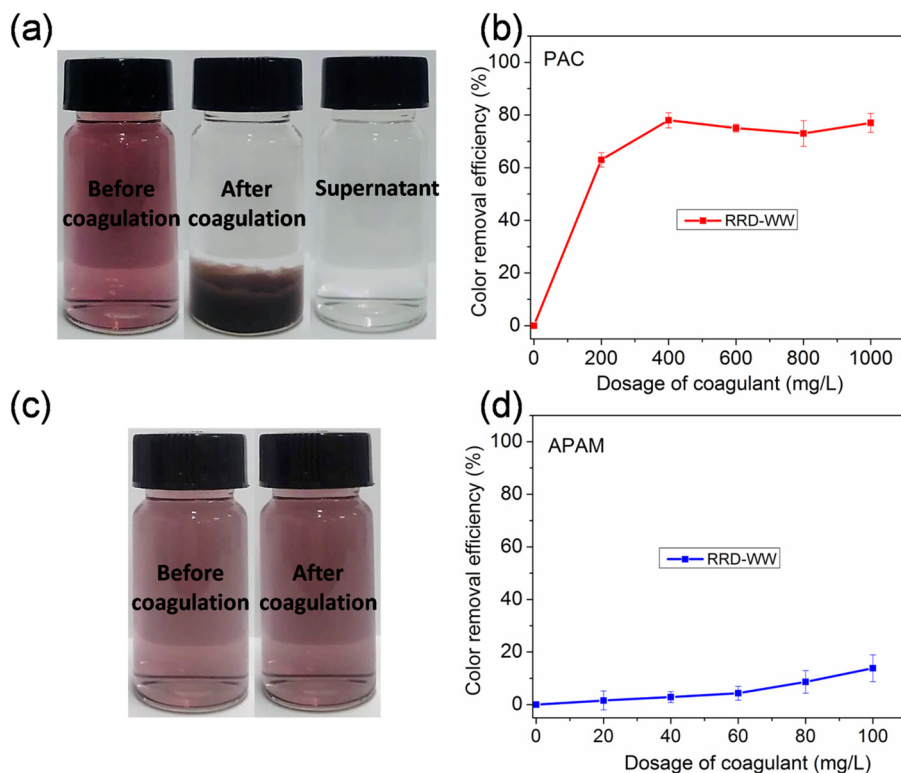


Fig. 8. Color removal of real raw reactive dyes wastewater by coagulation.

interests or personal relationships that could have appeared to influence the work reported in this paper.

Acknowledgements

This work was supported by the National Natural Science Foundation of China (NSFC) (No. 21876025) and the National water pollution control key project (2017ZX07202005-005).

Appendix A. Supplementary data

Supplementary data to this article can be found online at <https://doi.org/10.1016/j.cej.2020.126674>.

References

- H. Hayat, Q. Mahmood, A. Pervez, Z.A. Bhatti, S.A. Baig, Comparative decolorization of dyes in textile wastewater using biological and chemical treatment, *Sep. Purif. Technol.* 154 (2015) 149–153, <https://doi.org/10.1016/j.seppur.2015.09.025>.
- T.S. Pessôa, L.E. de Lima Ferreira, M.P. da Silva, L.M. Pereira Neto, B.F. do Nascimento, T.J.M. Fraga, E.F. Jaguaribe, J.V. Cavalcanti, M.A. da Motta Sobrinho, Açai waste benefiting by gasification process and its employment in the treatment of synthetic and raw textile wastewater, *J. Clean. Prod.* 240 (2019) 118047, <https://doi.org/10.1016/j.jclepro.2019.118047>.
- C.R. Holkar, A.J. Jadhav, D.V. Pinjari, N.M. Mahamuni, A.B. Pandit, A critical review on textile wastewater treatments: Possible approaches, *J. Environ. Manage.* 182 (2016) 351–366, <https://doi.org/10.1016/j.jenvman.2016.07.090>.
- C.M.B. de Araújo, G.F. Oliveira do Nascimento, G.R. Bezerra da Costa, A.M.S. Baptista, T.J.M. Fraga, R.B. de Assis Filho, M.G. Ghislandi, M.A. da Motta Sobrinho, Real textile wastewater treatment using nano graphene-based materials: Optimum pH, dosage, and kinetics for colour and turbidity removal, *Can. J. Chem. Eng.* 98 (2020) 1429–1440, <https://doi.org/10.1002/cjce.23712>.
- S. Sadri Moghaddam, M.R. Alavi Moghaddam, M. Arami, Coagulation/flocculation process for dye removal using sludge from water treatment plant: Optimization through response surface methodology, *J. Hazard. Mater.* 175 (2010) 651–657, <https://doi.org/10.1016/J.JHAZMAT.2009.10.058>.
- A.Y. Zahrim, N. Hilal, Treatment of highly concentrated dye solution by coagulation/flocculation–sand filtration and nanofiltration, *Water Resour. Ind.* 3 (2013) 23–34, <https://doi.org/10.1016/J.WRI.2013.06.001>.
- N.H. Torres, B.S. Souza, L.F.R. Ferreira, Á.S. Lima, G.N. dos Santos, E.B. Cavalcanti, Real textile effluents treatment using coagulation/flocculation followed by electrochemical oxidation process and ecotoxicological assessment, *Chemosphere.* 236 (2019) 124309, <https://doi.org/10.1016/j.chemosphere.2019.07.040>.
- E. Bazrafshan, M.R. Alipour, A.H. Mahvi, Textile wastewater treatment by application of combined chemical coagulation, electrocoagulation, and adsorption processes, *Desalin. Water Treat.* 57 (2016) 9203–9215, <https://doi.org/10.1080/19443994.2015.1027960>.
- M. Erkanlı, L. Yılmaz, P.Z. Çulfaz-Emecen, U. Yetis, Brackish water recovery from reactive dyeing wastewater via ultrafiltration, *J. Clean. Prod.* 165 (2017) 1204–1214, <https://doi.org/10.1016/j.jclepro.2017.07.195>.
- K. Yu, S. Yang, C. Liu, H. Chen, H. Li, C. Sun, S.A. Boyd, Degradation of Organic Dyes via Bismuth Silver Oxide Initiated Direct Oxidation Coupled with Sodium Bismuthate Based Visible Light Photocatalysis, *Environ. Sci. Technol.* 46 (2012) 7318–7326, <https://doi.org/10.1021/es3001954>.
- S. Karthikeyan, A. Titus, A. Gnanamani, A.B. Mandal, G. Sekaran, Treatment of textile wastewater by homogeneous and heterogeneous Fenton oxidation processes, *Desalination.* 281 (2011) 438–445, <https://doi.org/10.1016/J.DESAL.2011.08.019>.
- I. Khouni, B. Marrot, P. Moulin, R. Ben Amar, Decolorization of the reconstituted textile effluent by different process treatments: Enzymatic catalysis, coagulation/flocculation and nanofiltration processes, *Desalination.* 268 (2011) 27–37, <https://doi.org/10.1016/J.DESAL.2010.09.046>.
- F.O. Mcyotto, Q. Wei, C.W.K. Chow, Z. Nadeem, Z. Li, J. Liu, Eco-friendly decolorization of cationic dyes by coagulation using natural coagulant Bentonite and biodegradable flocculant Sodium Alginate, *SDRP J. Earth Sci. Environ. Stud.* 5 (2020) 51–60, <https://doi.org/10.25177/jeses.5.2.ra.10648>.
- S. Şahinkaya, COD and color removal from synthetic textile wastewater by ultrasound assisted electro-Fenton oxidation process, *J. Ind. Eng. Chem.* 19 (2013) 601–605, <https://doi.org/10.1016/J.JIEC.2012.09.023>.
- Y. Anjaneyulu, N. Sreedhara Chary, D. Samuel Suman Raj, Decolorization of Industrial Effluents – Available Methods and Emerging Technologies – A Review, *Rev. Environ. Sci. Bio/Technology.* 4 (2005) 245–273, <https://doi.org/10.1007/s1157-005-1246-z>.
- E. Ellouze, N. Tahri, R. Ben Amar, Enhancement of textile wastewater treatment process using Nanofiltration, *Desalination.* 286 (2012) 16–23, <https://doi.org/10.1016/J.DESAL.2011.09.025>.
- O. Türgan, G. Ersöz, S. Atalay, J. Fors, U. Welander, The treatment of azo dyes found in textile industry wastewater by anaerobic biological method and chemical oxidation, *Sep. Purif. Technol.* 79 (2011) 26–33, <https://doi.org/10.1016/J.SEPPUR.2011.03.007>.
- R.G. Saratale, G.D. Saratale, J.S. Chang, S.P. Govindwar, Bacterial decolorization and degradation of azo dyes: A review, *J. Taiwan Inst. Chem. Eng.* 42 (2011) 138–157, <https://doi.org/10.1016/J.JTICE.2010.06.006>.
- Y. Wei, A. Ding, L. Dong, Y. Tang, F. Yu, X. Dong, Characterisation and coagulation performance of an inorganic coagulant-poly-magnesium-silicate-chloride in treatment of simulated dyeing wastewater, *Colloids Surfaces A Physicochem. Eng. Asp.* 470 (2015) 137–141, <https://doi.org/10.1016/j.colsurfa.2015.01.066>.
- P. Arulmathi, C. Jeyaprabha, P. Sivasankar, V. Rajkumar, Treatment of Textile Wastewater by Coagulation-Flocculation Process Using Gossypium herbaceum and Polyaniline Coagulants, *Clean - Soil, Air, Water.* 47 (2019) 1800464, <https://doi.org/10.1002/clen.201800464>.
- M.C. Collivignarelli, A. Abbà, M. Carnevale Miino, S. Damiani, Treatments for color removal from wastewater: State of the art, *J. Environ. Manage.* (2019) 727–745, <https://doi.org/10.1016/j.jenvman.2018.11.094>.
- A.K. Verma, R.R. Dash, P. Bhunia, A review on chemical coagulation/flocculation technologies for removal of colour from textile wastewaters, *J. Environ. Manage.* 93 (2012) 154–168, <https://doi.org/10.1016/J.JENVMAN.2011.09.012>.
- A. Ahmad, S.H. Mohd-Setapar, C.S. Chuong, A. Khatoon, W.A. Wani, R. Kumar, M. Rafatullah, Recent advances in new generation dye removal technologies: Novel search for approaches to reprocess wastewater, *RSC Adv.* 5 (2015) 30801–30818, <https://doi.org/10.1039/c4ra16959j>.
- C.Y. Teh, P.M. Budiman, K.P.Y. Shak, T.Y. Wu, Recent Advancement of Coagulation-Flocculation and Its Application in Wastewater Treatment, *Ind. Eng. Chem. Res.* 55 (2016) 4363–4389, <https://doi.org/10.1021/acs.iecr.5b04703>.
- T. Peik-See, A. Pandikumar, L.H. Ngee, H.N. Ming, C.C. Hua, Magnetically separable reduced graphene oxide/iron oxide nanocomposite materials for environmental remediation, *Catal. Sci. Technol.* 4 (2014) 4396–4405, <https://doi.org/10.1039/C4CY00806E>.
- H. Zhuang, J. Guo, X. Hong, Advanced treatment of paper-making wastewater using catalytic ozonation with waste rice straw-derived activated carbon-supported manganese oxides as a novel and efficient catalyst, *Polish J. Environ. Stud.* 27 (2018) 451–457.
- S.N. Malik, P.C. Ghosh, A.N. Vaidya, S.N. Mudliar, Catalytic ozone pretreatment of complex textile effluent using Fe²⁺ and zero valent iron nanoparticles, *J. Hazard. Mater.* 357 (2018) 363–375, <https://doi.org/10.1016/j.jhazmat.2018.05.070>.
- M.C. Collivignarelli, A. Abbà, G. Bertanza, G. Barbieri, Treatment of high strength aqueous wastes in a thermophilic aerobic membrane reactor (TAMR): Performance and resilience, *Water Sci. Technol.* 76 (2017) 3236–3245, <https://doi.org/10.2166/wst.2017.492>.
- K. Meerbergen, K.A. Willems, R. Dewil, J. Van Impe, L. Appels, B. Lievens, Isolation and screening of bacterial isolates from wastewater treatment plants to decolorize azo dyes, *J. Biosci. Bioeng.* 125 (2018) 448–456, <https://doi.org/10.1016/j.jbiosc.2017.11.008>.
- A. Ghosh, M.G. Dastidar, T.R. Sreekrishnan, Bioremediation of Chromium Complex Dye by Growing *Aspergillus flavus*, *Water Quality Management, Water Sci. Technol. Library* 79 (2018) 81–92, https://doi.org/10.1007/978-981-10-5795-3_8.
- M. Ajaz, A. Elahi, A. Rehman, Degradation of azo dye by bacterium, *Alishewanella* sp. CBL-2 isolated from industrial effluent and its potential use in decontamination of wastewater, *J. Water Reuse Desalin.* 8 (2018) 507–515, <https://doi.org/10.2166/wrd.2018.065>.
- H. Zhang, X. Zhang, A. Geng, Expression of a novel manganese peroxidase from *Cerrena unicolor* BBP6 in *Pichia pastoris* and its application in dye decolorization and PAH degradation, *Biochem. Eng. J.* 153 (2020) 107402, <https://doi.org/10.1016/j.bej.2019.107402>.
- X. Pang, L. Sellaoui, D. Franco, G.L. Dotto, J. Georjina, A. Bajahzar, H. Belmabrouk, A. Ben Lamine, A. Bonilla-Petriciolet, Z. Li, Adsorption of crystal violet on bio-masses from pecan nutshell, para chestnut husk, araucaria bark and palm cactus: Experimental study and theoretical modeling via monolayer and double layer statistical physics models, *Chem. Eng. J.* 378 (2019) 122101, <https://doi.org/10.1016/j.cej.2019.122101>.
- L. Fu, C. Shuang, F. Liu, A. Li, Y. Li, Y. Zhou, H. Song, Rapid removal of copper with magnetic poly-acrylic weak acid resin: Quantitative role of bead radius on ion exchange, *J. Hazard. Mater.* 272 (2014) 102–111, <https://doi.org/10.1016/J.JHAZMAT.2014.02.047>.
- M.M. Hassan, C.M. Carr, A critical review on recent advancements of the removal of reactive dyes from dyehouse effluent by ion-exchange adsorbents, *Chemosphere.* 209 (2018) 201–219, <https://doi.org/10.1016/j.chemosphere.2018.06.043>.
- X. Duan, P. Wu, K. Pi, H. Zhang, D. Liu, A.R. Gerson, Application of modified electrocoagulation for efficient color removal from synthetic methylene blue wastewater, *Int. J. Electrochem. Sci.* 13 (2018) 5575–5588.
- X. Wei, X. Kong, S. Wang, H. Xiang, J. Wang, J. Chen, Removal of Heavy Metals from Electroplating Wastewater by Thin-Film Composite Nanofiltration Hollow-Fiber Membranes, *Ind. Eng. Chem. Res.* 52 (2013) 17583–17590, <https://doi.org/10.1021/ie402387u>.
- C.X.H. Su, L.W. Low, T.T. Teng, Y.S. Wong, Combination and hybridisation of treatments in dye wastewater treatment: A review, *J. Environ. Chem. Eng.* 4 (2016) 3618–3631, <https://doi.org/10.1016/j.jece.2016.07.026>.
- G. Boczkaj, A. Fernandes, Wastewater treatment by means of advanced oxidation processes at basic pH conditions: A review, *Chem. Eng. J.* 320 (2017) 608–633, <https://doi.org/10.1016/j.cej.2017.03.084>.
- F. İlhan, K. Ulucan-Altuntas, C. Dogan, U. Kurt, Treatability of raw textile wastewater using Fenton process and its comparison with chemical coagulation, *Desalin. Water Treat.* 162 (2019) 142–148, <https://doi.org/10.5004/dwt.2019.24332>.
- C. Fersi, M. Dhahbi, Treatment of textile plant effluent by ultrafiltration and/or nanofiltration for water reuse, *Desalination.* 222 (2008) 263–271, <https://doi.org/10.1016/J.DESAL.2007.01.171>.

- [42] P. Fongsatitkul, P. Elefsiniotis, A. Yamasmith, N. Yamasmith, Use of sequencing batch reactors and Fenton's reagent to treat a wastewater from a textile industry, *Biochem. Eng. J.* 21 (2004) 213–220, <https://doi.org/10.1016/J.BEJ.2004.06.009>.
- [43] A. Srinivasan, T. Viraraghavan, Decolorization of dye wastewaters by biosorbents: A review, *J. Environ. Manage.* 91 (2010) 1915–1929, <https://doi.org/10.1016/J.JENVMAN.2010.05.003>.
- [44] A. Yadav, S. Mukherji, A. Garg, Removal of chemical oxygen demand and color from simulated textile wastewater using a combination of chemical/physicochemical processes, *Ind. Eng. Chem. Res.* 52 (2013) 10063–10071, <https://doi.org/10.1021/ie400855b>.
- [45] F.C. Moreira, R.A.R. Boaventura, E. Brillas, V.J.P. Vilar, Electrochemical advanced oxidation processes: A review on their application to synthetic and real wastewaters, *Appl. Catal. B Environ.* 202 (2017) 217–261, <https://doi.org/10.1016/j.apcatb.2016.08.037>.
- [46] G. Asadollahfardi, H. Zangooei, V. Motamedi, M. Davoodi, Selection of coagulant using jar test and analytic hierarchy process: A case study of Mazandaran textile wastewater, *Adv. Environ. Res.* 7 (2018) 1–11.
- [47] B.H. Tan, T.T. Teng, A.K.M. Omar, Removal of dyes and industrial dye wastes by magnesium chloride, *Water Res.* 34 (2000) 597–601, [https://doi.org/10.1016/S0043-1354\(99\)00151-7](https://doi.org/10.1016/S0043-1354(99)00151-7).
- [48] B.-Y. Gao, Y. Wang, Q.-Y. Yue, J.-C. Wei, Q. Li, Color removal from simulated dye water and actual textile wastewater using a composite coagulant prepared by polyferric chloride and polydimethylallylammonium chloride, *Sep. Purif. Technol.* 54 (2007) 157–163, <https://doi.org/10.1016/J.SEPPUR.2006.08.026>.
- [49] J.Q. Jiang, N.J.D. Graham, Enhanced Coagulation Using Al/Fe(III) Coagulants: Effect of Coagulant Chemistry on the Removal of Colour-Causing NOM, *Environ. Technol.* 17 (1996) 937–950, <https://doi.org/10.1080/09593330.1996.9618422>.
- [50] L. Tang, F. Xiao, Q. Wei, Y. Liu, Y. Zou, J. Liu, W. Sand, C. Chow, Removal of active dyes by ultrafiltration membrane pre-deposited with a PSFM coagulant: Performance and mechanism, *Chemosphere.* 223 (2019) 204–210, <https://doi.org/10.1016/J.CHEMOSPHERE.2019.02.034>.
- [51] C.Z. Liang, S.P. Sun, F.Y. Li, Y.K. Ong, T.S. Chung, Treatment of highly concentrated wastewater containing multiple synthetic dyes by a combined process of coagulation/flocculation and nanofiltration, *J. Memb. Sci.* 469 (2014) 306–315, <https://doi.org/10.1016/j.memsci.2014.06.057>.
- [52] Y. Sun, S. Zhou, P.-C. Chiang, K.J. Shah, Evaluation and optimization of enhanced coagulation process: Water and energy nexus, *Water-Energy Nexus.* 2 (2019) 25–36, <https://doi.org/10.1016/j.wen.2020.01.001>.
- [53] A. Matilainen, N. Lindqvist, T. Tuhkanen, Comparison of the Efficiency of Aluminium and Ferric Sulphate in the Removal of Natural Organic Matter During Drinking Water Treatment Process, *Environ. Technol.* 26 (2005) 867–876, <https://doi.org/10.1080/09593332608618502>.
- [54] Y. Yu, Y.-Y. Zhuang, Y. Li, M.-Q. Qiu, Effect of Dye Structure on the Interaction between Organic Flocculant PAN-DCD and Dye, *Ind. Eng. Chem. Res.* 41 (2002) 1589–1596, <https://doi.org/10.1021/ie010745t>.
- [55] F. El-Gohary, A. Tawfik, Decolorization and COD reduction of disperse and reactive dyes wastewater using chemical-coagulation followed by sequential batch reactor (SBR) process, *Desalination.* 249 (2009) 1159–1164, <https://doi.org/10.1016/j.desal.2009.05.010>.
- [56] P. Cañizares, F. Martínez, C. Jiménez, J. Lobato, M. Rodrigo, Coagulation and Electrocoagulation of Wastes Polluted with Dyes, *Environ. Sci. Technol.* 40 (2006) 6418–6424, <https://doi.org/10.1021/ES0608390>.
- [57] B. Gao, Q. Yue, J. Miao, Evaluation of polyaluminium ferric chloride (PAFC) as a composite coagulant for water and wastewater treatment, *Water Sci. Technol.* 47 (2003) 127–132.
- [58] B.-Y. Gao, Q.-Y. Yue, Y. Wang, W.-Z. Zhou, Color removal from dye-containing wastewater by magnesium chloride, *J. Environ. Manage.* 82 (2007) 167–172, <https://doi.org/10.1016/j.jenvman.2005.12.019>.
- [59] W. Chu, Dye Removal from Textile Dye Wastewater Using Recycled Alum Sludge, *Water Res.* 35 (2001) 3147–3152, [https://doi.org/10.1016/S0043-1354\(01\)00015-X](https://doi.org/10.1016/S0043-1354(01)00015-X).
- [60] Q. Wang, Z. Luan, N. Wei, J. Li, C. Liu, The color removal of dye wastewater by magnesium chloride/red mud (MRM) from aqueous solution, *J. Hazard. Mater.* 170 (2009) 690–698, <https://doi.org/10.1016/J.JHAZMAT.2009.05.011>.
- [61] M. Zonoozi, M. Moghaddam, M. Arami, Coagulation/flocculation of dye-containing solutions using polyaluminium chloride and alum, *Water Sci. Technol.* 59 (2009) 1343–1351, <https://doi.org/10.2166/wst.2009.128>.
- [62] B. Bolto, J. Gregory, Organic polyelectrolytes in water treatment, *Water Res.* 41 (2007) 2301–2324, <https://doi.org/10.1016/j.watres.2007.03.012>.
- [63] C.S. Lee, J. Robinson, M.F. Chong, A review on application of flocculants in wastewater treatment, *Process Saf. Environ. Prot.* 92 (2014) 489–508, <https://doi.org/10.1016/j.psep.2014.04.010>.
- [64] M. Joshi, R. Bansal, R. Purwar, Colour removal from textile effluents, *Indian J. of Fibre and Textile Research.* 29 (2004) 239–259. http://nopr.niscair.res.in/bitstream/123456789/24631/1/IJFTR_29%2829%29_239-259.pdf (accessed 3 September 2019).
- [65] Y. You, X. Sun, W. Yang, L. Dai, L. He, H. Wang, J. Zhang, W. Xiang, A high-performance and low-cost strategy to harvest saltwater *Chlorella vulgaris* using cationic polyacrylamide coupled with bentonite, *Algal Res.* 41 (2019) 101579, <https://doi.org/10.1016/j.algal.2019.101579>.
- [66] Q.Y. Yue, B.Y. Gao, Y. Wang, H. Zhang, X. Sun, S.G. Wang, R.R. Gu, Synthesis of polyamine flocculants and their potential use in treating dye wastewater, *J. Hazard. Mater.* 152 (2008) 221–227, <https://doi.org/10.1016/j.jhazmat.2007.06.089>.
- [67] A. Kumar, C.K. Dixit, Methods for characterization of nanoparticles, *Adv. Nanomedicine Deliv. Ther. Nucleic Acids.* (2017) 44–58, <https://doi.org/10.1016/B978-0-08-100557-6.00003-1>.
- [68] A.Z. Bouyakoub, B.S. Lartiges, R. Ouhib, S. Kacha, A.G. El Samrani, J. Ghanbaja, O. Barres, MnCl₂ and MgCl₂ for the removal of reactive dye Levafix Brilliant Blue EBRA from synthetic textile wastewaters: An adsorption/aggregation mechanism, *J. Hazard. Mater.* 187 (2011) 264–273, <https://doi.org/10.1016/j.jhazmat.2011.01.008>.
- [69] L. Liu, C. Wu, Y. Chen, H. Wang, Preparation, characterization and coagulation behaviour of polyferric magnesium silicate (PFMSi) coagulant, *Water Sci. Technol.* 75 (2017) 1961–1970, <https://doi.org/10.2166/wst.2017.087>.
- [70] J. Leentvaar, M. Rebhun, Effect of magnesium and calcium precipitation on coagulation-flocculation with lime, *Water Res.* 16 (1982) 655–662, [https://doi.org/10.1016/0043-1354\(82\)90087-2](https://doi.org/10.1016/0043-1354(82)90087-2).
- [71] B. Shi, G. Li, D. Wang, C. Feng, H. Tang, Removal of direct dyes by coagulation: The performance of preformed polymeric aluminum species, *J. Hazard. Mater.* 143 (2007) 567–574, <https://doi.org/10.1016/j.jhazmat.2006.09.076>.